

Three-dimensional carbon cloth-supported ZnO nanorod arrays as a binder-free anode for lithium-ion batteries

Lanyan Huang · Xin Wang · Fuxing Yin ·
Chengwei Zhang · Jinwei Gao · Junming Liu ·
Guofu Zhou · Yongguang Zhang ·
Zhumabay Bakenov

Received: 7 July 2016 / Accepted: 4 January 2017 / Published online: 30 January 2017
© Springer Science+Business Media Dordrecht 2017

Abstract Three-dimensional ZnO nanorod arrays on flexible high surface area carbon cloth were successfully synthesized and directly used as negative electrodes for lithium-ion batteries without using any binder additive. The structure and morphology of the as-prepared hybrid ZnO electrode were characterized by X-ray diffraction (XRD), scanning electron microscopy (SEM), and high-resolution transmission electron microscopy (HRTEM). When tested as anodes in a lithium cell, the hybrid electrode demonstrated a high discharge capacity along

with excellent rate capability and good cycling stability, delivering a reversible capacity of 891 mAh g^{-1} at the second cycle and retaining a capacity of 469 mAh g^{-1} after 100 cycles.

Keywords Lithium-ion battery · ZnO nanorods · Carbon cloth · Binder-free ZnO anode · Energy storage

Introduction

Nowadays, various types of energy conversion and storage devices such as solar cells, fuel cells, lithium-ion batteries (LIBs), and supercapacitors have received considerable attention as a result of the ever-growing demand for clean and renewable energy. Due to their high-energy density and excellent cyclic performance, LIBs are identified as the most promising candidates for power supply for a wide range of applications such as portable electronics, electric vehicles, and renewable energy storage (Wang et al. 2013). Commercial graphite anode is traditionally used as anode for LIBs because of its electrochemical and mechanical stability. However, graphite has a low specific capacity of 372 mAh g^{-1} (a theoretical value), which can hardly meet current increasing demands of LIBs with an enhanced energy-storing capacity (Xue et al. 2011).

The metal oxides (MO, $M = \text{Cu, Sn, Fe, Ni, Co, Zn}$) have higher theoretical capacity compared with the graphite anode, and thus were extensively studied as promising alternatives of graphite (Poizot et al. 2000; Wang et al. 2011; Wang et al. 2012). ZnO has been

L. Huang · X. Wang (✉) · G. Zhou
Institute of Electronic Paper Displays, South China Academy of
Advanced Optoelectronics, South China Normal University,
Guangdong Province, Guangzhou, China
e-mail: wangxin@sclu.edu.cn

F. Yin · Y. Zhang · Z. Bakenov
Synergy Innovation Institute of GDUT, Guangdong Province,
Heyuan, China

F. Yin · C. Zhang · Y. Zhang (✉)
Research Institute for Energy Equipment Materials, Tianjin Key
Laboratory of Materials Laminating Fabrication and Interface
Control Technology, Hebei University of Technology,
Tianjin 300130, China
e-mail: yongguangzhang@hebut.edu.cn

Z. Bakenov
Institute of Batteries LLC, National Laboratory Astana,
Nazarbayev University, 53 Kabanbay Batyr Avenue, Astana,
Kazakhstan 010000

L. Huang · J. Gao · J. Liu
Institute of Advanced Materials, South China Academy of
Advanced Optoelectronics, South China Normal University,
Guangdong Province, Guangzhou, China

considered as an excellent anode material due to its advantages of attractive theoretical capacity of 978 mAh g^{-1} , low cost, environmental friendliness, and a high chemical stability (Zhou et al. 2012; Wang et al. 2015). However, ZnO electrodes usually suffer from their intrinsic low electrical conductivity and large volume changes upon cycling, resulting in poor rate performance and mechanical disintegration (Fu et al. 2003; Woo et al. 2011; Park et al. 2013). In order to overcome these challenges, advanced design and development of facile synthesis routes for ZnO as anode for highly reversible and high-rate lithium storage are required.

Among a variety of potential strategies to achieve these goals, growing nanostructured electroactive materials directly on conductive substrates attracted interest and some preliminary results of such approach were reported recently (Huang et al. 2011; Pan et al. 2014). Nanostructured ZnO materials grown directly on the current collectors have been studied as novel carbon and binder-free electrodes for LIBs (Wang et al. 2009; Huang et al. 2011). Such nanostructured ZnO materials, including nanowires, nanosheets, or nanorods, provide a larger interphase area for electrode processes and a shorter charge transport distances (Wang et al. 2009; Hieu et al. 2012). Direct growth of electroactive materials on a current collector enhances the electric contact, promotes processes at the electrode/electrolyte interfaces, and suppresses the volume variations during discharge-charge process (Lou et al. 2013). Therefore, the electroactive materials directly grown on conductive substrates often exhibit better electrochemical performance than the electrodes coated by a common slurry pasting technique.

In this work, ZnO nanorods were grown vertically on three-dimensional (3D) flexible carbon cloth (designated as ZnO/CC) to form a binder-free electrode via a facile and scalable hydrothermal method. Such unique 3D nanostructure offers various inherent advantages such as high electric conductivity along with remarkable mechanical strength and excellent corrosion resistance. Furthermore, carbon cloth covered with 3D vertical ZnO nanorods allows for considerably large contact area with the electrolyte and more surface sites available for reversible reactions with lithium ions. Finally, the use of a binder-free anode, along with its reduced weight and increased active electrode material content, eliminates the demand for both conductive and binder additives,

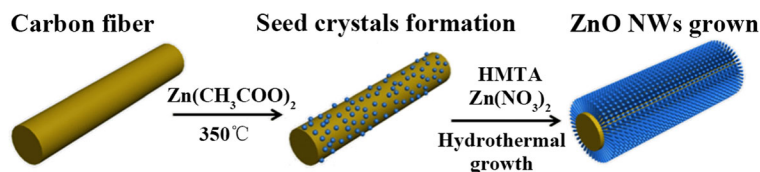
which simplifies the electrode fabrication and remarkably reduces its cost (Pan et al. 2014; Chen et al. 2015).

Experimental

As shown in Scheme 1, well-aligned ZnO nanorods were grown on a flexible 3D carbon cloth via a modified two-step hydrothermal synthetic method (Greene et al. 2005). Before use, the carbon cloth was washed several times with acetone and ethanol and then dried at $80 \text{ }^\circ\text{C}$ in a dryer. Further, the working solution of $5 \text{ mM Zn (CH}_3\text{COO)}_2$ (99%, Sigma) in ethanol was added dropwise to carbon cloth substrate, and the system was dried by blowing nitrogen gas. This step was repeated three to five times, and the carbon cloth coated with ZnO seed layer was obtained after annealing at $350 \text{ }^\circ\text{C}$ for 20 minutes. The layer was further hydrothermally grown at $90 \text{ }^\circ\text{C}$ for 3 h by sealing the substrate in 100 mL growth solution composed of zinc nitrate hydrate (25 mM, $\text{Zn (NO}_3)_2 \cdot 6\text{H}_2\text{O}$, 99%, National Medicine) and methenamine (25 mM, 99%, National Medicine). The resulting sample was rinsed several times with deionized water and dried at room temperature to obtain the ZnO nanorod arrays on carbon cloth electrode.

X-ray diffraction (XRD, Bruker D8 advance with Cu $K\alpha$ radiation) was used to analyze the crystalline structure of the samples. The morphology and structure of the samples were characterized by field emission scanning electron microscopy (FE-SEM, S4800, Hitachi Limited) and transmission electron microscopy (TEM, JEM-2100F, JEOL), respectively.

Coin-type cells (CR2025) were assembled in a glove box (MBraun) filled with argon gas (99.9995%) and used for electrochemical measurements. The as-prepared ZnO nanorod arrays on carbon cloth were used directly as a binder-free working electrode. Lithium metal foil served as both a reference and counter electrode. Electrodes were separated by a microporous polypropylene membrane (Celgard 2300) soaked in the electrolyte, which was a solution of 1 M LiPF_6 in a mixture of dimethyl carbonate, diethyl carbonate, and ethylene carbonate (1:1:1 in weight). The ZnO active material loading in each electrode was about 1.5 mg cm^{-2} . Cells were sealed in a glove box and aged for 12 h before electrochemical measurements. A battery tester (LAND CT2001A) was used to investigate the discharge/charge cycling performances of the cells at different current densities between 0.005 and $3 \text{ V vs. Li}^+/\text{Li}$. Cyclic



Scheme 1 A schematics of the preparation process of the ZnO nanorods' grown on carbon cloth

voltammetry (CV) was performed at a scan rate of 0.1 mV s^{-1} using Biologic VMP-3 potentiostat/galvanostat.

Results and discussion

The XRD patterns of the as-prepared ZnO/CC and the bare carbon cloth are shown in Fig. 1. The diffraction peaks of ZnO/CC at 31.7° , 34.4° , 36.2° , 47.5° , 56.6° , 62.8° , 66.4° , 67.9° , and 69.0° can be indexed as the (100), (002), (101), (102), (110), (103), (200), (112), and (201) crystal planes of wurtzite-type hexagonal ZnO (JCPDS No. 65-3411) (Li et al. 2016a). A strong (002) diffraction peak of ZnO/CC at 26.2° , which conforms with the bare carbon cloth, demonstrates that the ZnO crystals were successfully grown on the surface of carbon cloth substrate.

The SEM images in Fig. 2 present the morphology of the as-prepared ZnO/CC at different magnifications. It can be seen from Fig. 2a and b that the surface of the carbon cloth is populated with high-density and homogeneously arranged ZnO nanorods. From the magnified SEM images in Fig. 2c and d, one can see that the ZnO nanorods are quasi-vertically erected on the carbon cloth surface and have a uniform diameter distribution with

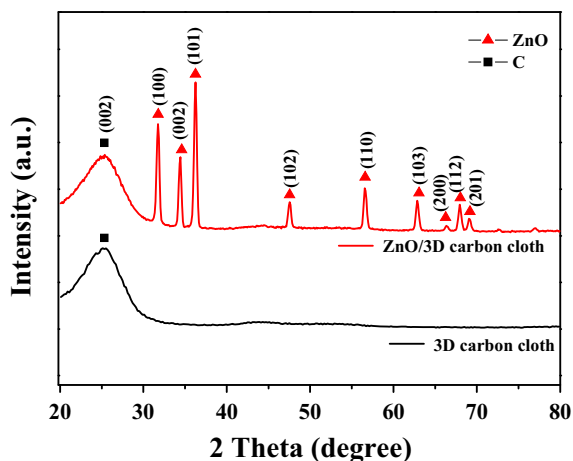


Fig. 1 XRD patterns of ZnO/CC and carbon cloth

the average value of about 80 nm (inset of Fig. 2d). The unique integrated ZnO nanorod architecture not only increases the contact area at the electrode and electrolyte interface but also accommodates the volume changes upon Li ions insertion/desertion processes and reduces its negative effect on the electrode performance (Yu et al. 2013; Li et al. 2016a).

The microstructure and crystalline structure of the ZnO/CC were further investigated by TEM. Figure 3a and b present typical ZnO nanorods with a diameter less than 100 nm and exhibits its nanostructure. The higher magnification TEM image (Fig. 3c) shows obvious lattice spacing of 0.261 nm, which corresponds well with the (002) lattice plane for hexagonal ZnO. Figure 3d shows the SAED patterns of ZnO nanorods, which confirms formation of well-defined monocrystalline ZnO particles.

CV measurements were performed to investigate the electrochemical behavior of the ZnO/CC nanocomposite electrodes (Fig. 4a). During the first cycle, a peak could be observed around 0.5 V vs. Li^+/Li , which can be attributed to the formation of a solid electrolyte interphase (SEI) layer and the conversion of ZnO to Zn metal (Belliard and Irvine 2001; Xie et al. 2014). Upon further cycling, the CV curves of ZnO/CC contain the reversible reduction and oxidation peaks inherent for this system (Ahmad et al. 2011). It can be seen that these cycles are characterized with the CV curves of the same shape, which are almost overlapping with each other, exhibiting excellent electrochemical reversibility.

The electrochemical performance of the ZnO/CC composite as an anode for lithium-ion battery was evaluated by galvanostatic cycling at a current density of 200 mA g^{-1} . The initial charge/discharge profiles of ZnO/CC anode are shown in Fig. 4b, and present typical features of ZnO-based anode materials (Wang et al. 2016). In the first discharge curve, one clear potential slope at 0.5–0.6 V can be observed and the overall discharge capacity was as high as 1379 mAh g^{-1} , which is associated with the inevitable formation of SEI and the reduction process of ZnO to Zn metal ($\text{ZnO} + 2\text{Li} \rightarrow \text{Zn} + \text{Li}_2\text{O}$) (Li et al. 2016b). In the following cycles, the

Fig. 2 a–d SEM microstructures of ZnO/CC at different magnification. Inset in d the diameter distribution of the ZnO nanorods

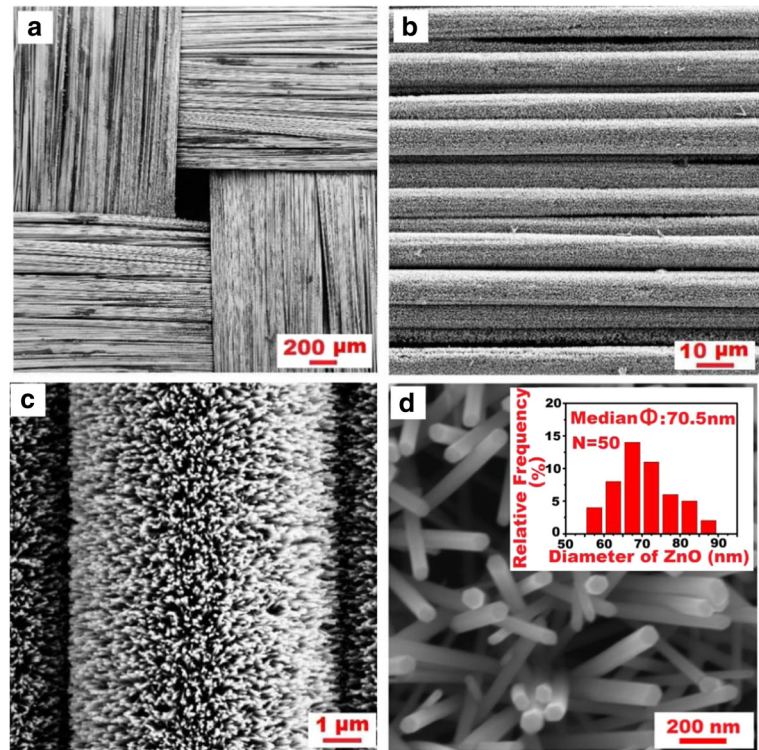
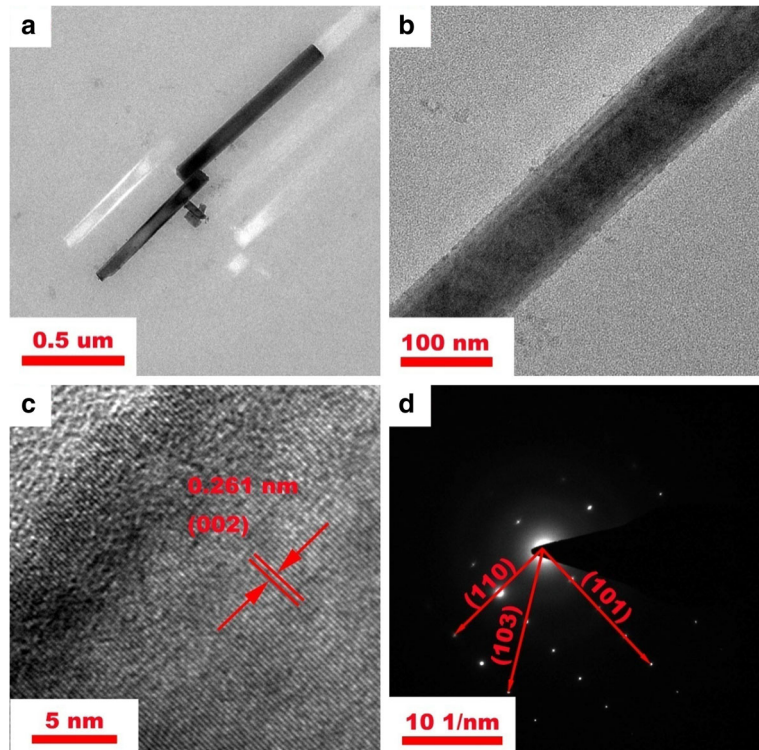


Fig. 3 a, b TEM images and c HRTEM image of the ZnO nanorods. d SAED patterns of the ZnO nanorods



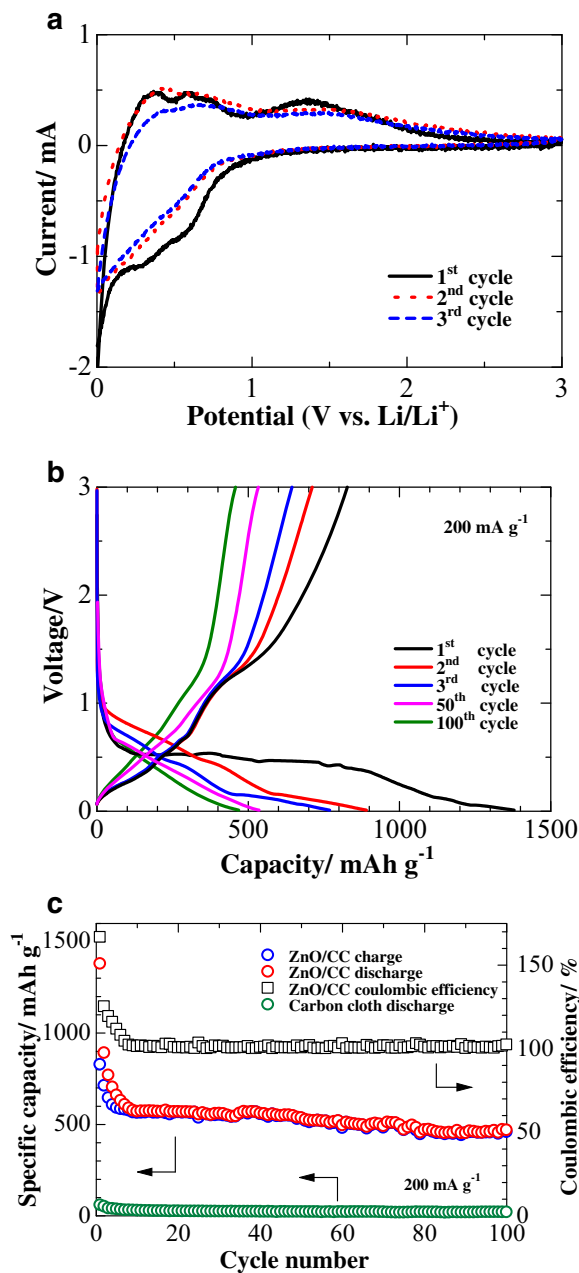


Fig. 4 **a** CV curves of lithium cell with ZnO/CC anode. **b** Galvanostatic discharge/charge profiles of the ZnO/CC anode at 200 mA g⁻¹. **c** Cycling performance of bare carbon cloth and ZnO/CC anode at 200 mA g⁻¹

discharge curve is different from the initial one, and indicates occurrence of different electrochemical reactions ($x\text{Li} + \text{Zn} \rightarrow \text{Li}_x\text{Zn}$). At the second discharge-charge process, the discharge and charge capacities were 891 and 712 mAh g⁻¹, respectively, with a coulombic

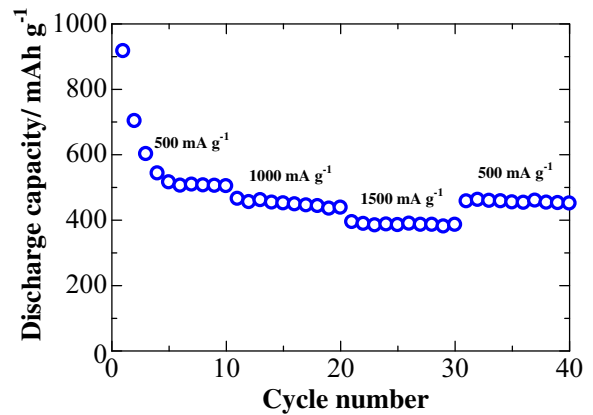


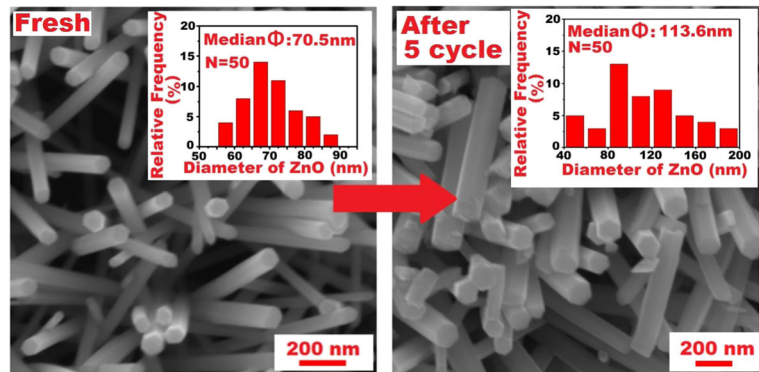
Fig. 5 Rate performance of the ZnO/CC anode

efficiency of 80%, which is much higher than that was observed at the first cycle (60%).

The cycling performance of the bare carbon cloth and ZnO/CC electrodes was studied at a current density of 200 mA g⁻¹ (0.3 mA cm⁻²) as shown in Fig. 4c. One can see that carbon cloth is electrochemically inactive within the studied potential region and thus, there are no noticeable capacity contribution in the ZnO/CC electrodes. Within a few initial cycles, the ZnO/CC anode exhibits a slight capacity decay. However, upon the following cycles, the cell capacity stabilizes, and about 53% of its initial reversible value (the second cycle capacity) could be retained over 100 cycles, indicating a good cycling performance of the anode. This enhanced reversibility of the system indicates that a highly ordered arrangement of ZnO nanorods perpendicularly to the carbon cloth substrate surface forms a stable structure and provides a larger interfacial/conducting area, boosting the electrochemical activity.

Figure 5 shows the rate capability data of the ZnO/CC anode at current densities of 500, 1000, and 1500 mA g⁻¹. For these measurements, 10 cycles were carried out at each current density. Although the reversible capacity gradually decreases with the increase in current density, the system still delivers a specific discharge capacity of 385 mAh g⁻¹ even at a high current density of 1500 mA g⁻¹. Furthermore, the specific capacity of electrode could be restored to its original value when the cycling current density was reduced back to 500 mA g⁻¹. These results show that the ZnO/CC anode prepared in this work possesses a good rate capability along with a high electrochemical stability. This performance enhancement could also be ascribed to the unique 3D architecture of the ZnO/CC anode, favoring

Fig. 6 SEM of the ZnO/CC anode before and after 5 charge/discharge cycles at 200 mA g⁻¹



both ionic and electronic conductivity. Furthermore, the free-standing feature of the ZnO/CC anode eliminates the use of binders in the cathode, and thereby avoids the unwanted conductivity impairment and energy loss caused by the resistance of binders. Consequently, this improves the electronic conductivity of the system, allowing for the high-rate charge/discharge operation (Xie et al. 2015).

In order to demonstrate the integrity maintenance of the ZnO/CC electrodes upon cycling, fresh electrode and one after 5 charge/discharge cycles at a current density of 200 mA g⁻¹ were investigated by SEM. Analysis of the micrographs obtained for the fresh and the cycled anodes (Fig. 6) confirms that both morphology and structure of the nanorods were retained upon cycling. The diameter increase of the nanorods (from 70 to 110 nm) is likely to be due to the huge volume change upon the charge/discharge processes.

Conclusions

In this work, ZnO nanorods with an average size of 80 nm were successfully grown on carbon cloth substrate via hydrothermal method. Due to the specific nanostructured and hierarchical 3D conductive pathway formed in the synthesized electrode, the as-prepared ZnO/CC anode presents a good cycling stability with a high capacity up to 469 mAh g⁻¹ at a current density of 200 mA g⁻¹ over 100 cycles, along with an enhanced rate capability allowing a delivery of a capacity of 385 mAh g⁻¹ even at a high current density of 1500 mA g⁻¹. The present study therefore indicates that this free-standing ZnO/CC could be considered as a promising anode for LIBs, and the strategy and concept

reported in the current work could inspire the further development of binder-free metal oxide anode for LIBs.

Acknowledgements The authors acknowledge the financial support from the NSFC Grant No. 21406052, 51602111, Guangdong Province Grant NO. 2014B090914004, 2014B090915005, 2015A030310196, 2015B050501010, 14KJ13, the Program for the Outstanding Young Talents of Hebei Province (Grant No. BJ2014010), the Pearl River S&T Nova Program of Guangzhou (201506040045), PCSIRT Project No. IRT13064 and Scientific Research Foundation for Selected Overseas Chinese Scholars, Ministry of Human Resources and Social Security of China (Grant No. CG2015003002). ZB acknowledges the financial support by the grants from the Ministry of Education and Science of Kazakhstan #5097/GF and 5687/GF.

Compliance with ethical standards

Conflict of interest The authors declare that they have no conflict of interest.

References

- Ahmad M, Shi Y, Nisar A, Sun H, Shen W, Wei M, Zhu J (2011) Synthesis of hierarchical flower-like ZnO nanostructures and their functionalization by Au nanoparticles for improved photocatalytic and high performance Li-ion battery anodes. *J Mater Chem* 2011:7723–7729
- Belliard F, Irvine JTS (2001) Electrochemical performance of ball-milled ZnO–SnO₂ systems as anodes in lithium-ion battery. *J Power Sources* 97–98(7):219–222
- Chen Y, Liu B, Jiang W, Liu Q, Liu J, Wang J, Zhang H, Jing X (2015) Coaxial three-dimensional CoMoO₄ nanowire arrays with conductive coating on carbon cloth for high-performance lithium ion battery anode. *J Power Sources* 300:132–138
- Fu ZW, Feng H, Ye Z, Yue C, Qin QZ (2003) The electrochemical reaction of zinc oxide thin films with lithium. *J Electrochem Soc* 150:A714–A720

- Greene LE, Law M, Tan DH, Montano M, Goldberger J, Somorjai G, Yang P (2005) General route to vertical ZnO nanowire arrays using textured ZnO seeds. *Nano Lett* 5:1231–1236
- Hieu NS, Lim JC, Lee JK (2012) Free-standing silicon nanorods on copper foil as anode for lithium-ion batteries. *Microelectron Eng* 89:138–140
- Huang XH, Xia XH, Yuan YF, Zhou F (2011) Porous ZnO nanosheets grown on copper substrates as anodes for lithium ion batteries. *Electrochim Acta* 56:4960–4965
- Li H, Wei Y, Zhang Y, Yin F, Zhang C, Wang G, Bakenov Z (2016a) Synthesis and electrochemical investigation of highly dispersed ZnO nanoparticles as anode material for lithium-ion batteries. *Ionics* 22:1387–1393
- Li H, Wei Y, Zhao Y, Zhang Y, Yin F, Zhang C, Bakenov Z (2016b) Simple one-pot synthesis of hexagonal ZnO nanoplates as anode material for lithium-ion batteries. *J Nanomater* 2016:4675960
- Lou F, Zhou H, Vullum-Bruer F, Tran TD, Chen D (2013) Synthesis of carbon nanofibers@MnO₂ 3D structures over copper foil as binder free anodes for lithium ion batteries. *J Energy Chem* 22:78–86
- Park KT, Xia F, Kim SW, Kim SB, Song T, Paik U, Park WI (2013) Facile synthesis of ultrathin ZnO nanotubes with well-organized hexagonal nanowalls and sealed layouts: applications for lithium ion battery anodes. *J Phys Chem C* 117:1037–1043
- Pan GX, Xia XH, Cao F, Chen J, Zhang YJ (2014) Carbon cloth supported vanadium pentaoxide nanoflake arrays as high-performance cathodes for lithium ion batteries. *Electrochim Acta* 149:349–354
- Poizot P, Laruelle S, Grugeon S, Dupont L, Tarascon JM (2000) ChemInform abstract: nano-sized transition-metal oxides as negative-electrode materials for lithium-ion batteries. *Nature* 407:496–499
- Wang B, Wang G, Zheng Z, Wang H, Bai JT, Bai JB (2013) Carbon coated Fe₃O₄ hybrid material prepared by chemical vapor deposition for high performance lithium-ion batteries. *Electrochim Acta* 106:235–243
- Wang Z, Luan D, Boey FY, Lou XW (2011) Fast formation of SnO₂ nanoboxes with enhanced lithium storage capability. *J Am Chem Soc* 133:4738–4741
- Wang Z, Luan D, Madhavi S, Hu Y, Lou XW (2012) Assembling carbon-coated α -Fe₂O₃ hollow nanohorns on the CNT backbone for superior lithium storage capability. *Energy Environ Sci* 5:5252–5256
- Wang L, Tang K, Zhang M, Xu J (2015) Facile synthesis of Mn-doped ZnO porous nanosheets as anode materials for lithium ion batteries with a better cycle durability. *Nanoscale Res Lett* 10:1–5
- Wang H, Pan Q, Cheng Y, Zhao J, Yin G (2009) Evaluation of ZnO nanorod arrays with dandelion-like morphology as negative electrodes for lithium-ion batteries. *Electrochim Acta* 54:2851–2855
- Wang X, Huang L, Zhao Y, Zhang Y, Zhou G (2016) Synthesis of mesoporous ZnO nanosheets via facile solvothermal method as the anode materials for lithium-ion batteries. *Nanoscale Res Lett* 11:37
- Woo MA, Kim TW, Kim IY, Hwang SJ (2011) Synthesis and lithium electrode application of ZnO-ZnFe₂O₄ nanocomposites and porously assembled ZnFe₂O₄ nanoparticles. *Solid State Ionics* 182:91–97
- Xie Q, Zhang X, Wu X (2014) Yolk-shell ZnO-C microspheres with enhanced electrochemical performance as anode material for lithium ion batteries. *Electrochim Acta* 125:659–665
- Xie X, Kretschmer K, Zhang J, Sun B, Su D, Wang G (2015) Sn@CNT nanopillars grown perpendicularly on carbon paper: a novel free-standing anode for sodium ion batteries. *Nano Energy* 13:208–217
- Xue XY, Chen ZH, Xing LL, Yuan S, Chen YJ (2011) SnO₂/ α -MoO₃ core-shell nanobelts and their extraordinarily high reversible capacity as lithium-ion battery anodes. *Chem Commun* 47:5205–5207
- Yu J, Du N, Wang J, Zhang H, Yang D (2013) SiGe porous nanorod arrays as high-performance anode materials for lithium-ion batteries. *J Alloys Compd* 577:564–568
- Zhou M, Hu Y, Liu Y, Yang W, Qian H (2012) Microwave-assisted route to fabricate coaxial ZnO/CdS nanocables with enhanced visible light-driven photocatalytic activity. *CrystEngComm* 14:7686–7693